AI-based handling of detector gaps in diagnostic photon-counting CT

Purpose

The trend in CT is towards higher spatial resolution and small pixel size. One example is photon-counting computed tomography (PCCT), which uses semiconductors in comparison to classic energy-integrating detectors (EIDs) to enable the direct transfer of X-ray photons into an electrical signal. This allows more detailed spectral information to be obtained, which can be used for virtual monoenergetic or multi-energy CT applications, for example [1].

However, smaller detector pixels also affect the structure of the detector. A fundamental component of detectors is the anti-scatter grid (ASG), which minimizes scattered radiation and thus prevents image artifacts. In EIDs, the ASG surrounds each detector pixel and ensures that the detector pixel centers are regularly spaced. In contrast, the ASG in the PCCT surrounds several grouped detector pixels due to the smaller pixel size and thus leads to irregularly arranged detector pixel centers (see Fig. 1). The ASG blocks primary radiation behind the lamellae, which can result in dead detector rows and columns. This regular pattern of dead rows and columns in the detector image must be inpainted to avoid possible artifacts in reconstructed images which may impair the diagnostic value of the images.

To this end, we present grid inpainting with deep learning (GRIDL), a deep learning-based approach to allow inpainting of gaps in column and row direction.

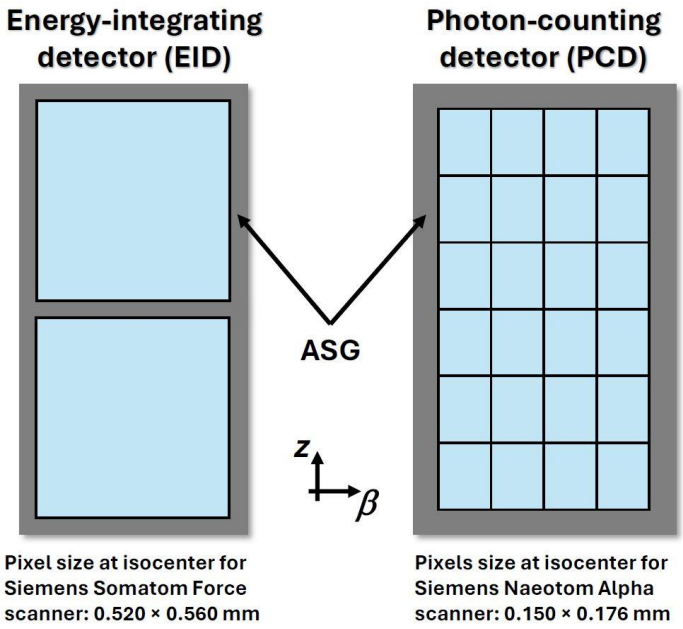

Figure 1: Layout comparison between energy-integrating and photon-counting detector.

Methods

Grid Inpainting with Deep Learning (GRIDL)

GRIDL consists of a comparable convolutional neural network as presented in [2, 3] and is trained in a supervised manner to learn a mapping between the corrupted input image and the corresponding pixels required to inpaint the gaps. A binary mask is used as additional network input to identify missing pixels within the input and to preserve existing parts of the image that should not be altered by the algorithm. The input layer is followed by 12 convolutional layers each with 128 filters, 3×3 kernels, stride 1×1, and zero padding. After network inference, the output is merged with the corrupted image to fill the corresponding gaps. In this experimental setup, gapless EID data were corrupted by artificial gap rows every six detector rows and gap columns every four detector columns, in a comparable way as the ASG would be arranged in a PCCT scanner.

Data Generation and Network Training

Network training used simulated projection data of randomly arranged spherical shells (diameter: 1 – 20 cm, density: 0.5 – 3.0 g/cm^3) within a water cylinder phantom [2] (see Fig. 2). In total 100 noise-free spiral CT scans with randomly arranged phantoms were simulated in EID geometry to obtain ground truth detector images without gaps. The projection data were corrupted using the outlined scheme of artificial gaps as shown in Figure 2. After initializing the corrupted projections by a linear interpolation random patches of size 32×32 were selected for training. The input consists of a patch from the initialized corrupted projection and the binary mask identifying the gaps while the corresponding patch from the gapless projection is used as ground truth. The training phase involved 500,000 patch pairs extracted from 80 scans for training and 125,000 patch pairs extracted from 20 scans for validation while minimizing a combined loss function integrating the mean absolute error and multi-scale similarity index.

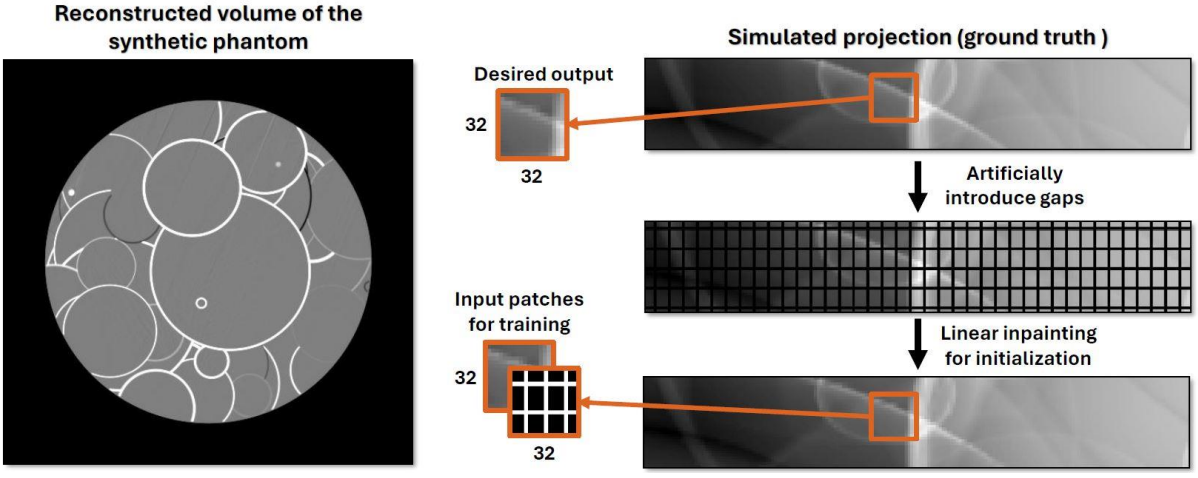

Figure 2: A reconstructed slice of the synthetic phantom and schematic representation of training patch generation for GRIDL.

Results

A qualitative and quantitative evaluation of GRIDL was performed in projection and image domain comparing it to traditional exemplar-based [4] and diffusion-based inpainting approaches [5, 6].

Projection Domain

Figure 3 shows the inpainting results of an exemplar-based and biharmonic diffusion-based inpainting approach compared to GRIDL using an artificially corrupted projection from a clinical head CT examination. When comparing the resulting projections visually almost no difference is visible between the three inpainting approaches compared. However, a closer examination reveals that several gaps are still visible after inpainting with the exemplar-based method. This becomes particularly visible when looking at the difference image to the gapless ground truth. The biharmonic diffusion-based inpainting and GRIDL yield visually superior results. From the difference images, neither of the two approaches can be favored in terms of better image quality. The root mean square error (RMSE) is also in a comparable range for both methods (Diffusion-based: 0.0057, GRIDL: 0.0059).

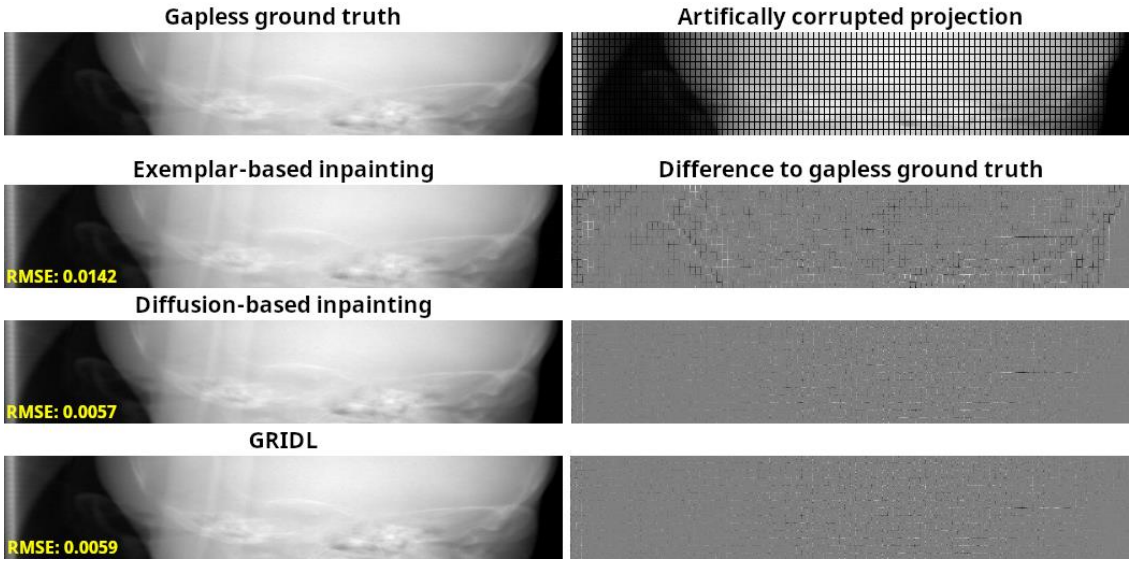

Figure 3: Inpainting results for an exemplar-based and diffusion-based inpainting approach compared to GRIDL using a clinical head CT projection.

Image Domain

Figure 4 shows a comparison of reconstructed slices of a head phantom scan. For this purpose, the projections of a CT scan in EID geometry were artificially corrupted by the outlined ASG-like gap pattern and then inpainted by the individual methods. A reconstruction of the gapless detector in the first column serves as ground truth. It is evident that the exemplar-based method leads to multiple aliasing and ring artifacts and thus achieves inferior image quality in this comparison. While biharmonic inpainting yields improved inpainting results, several aliasing artifacts remain in the eye cavity area. GRIDL provides superior image quality and best correlation with the gapless ground truth. This is underlined by a reduced RMSE and an improvement in the structural similarity index (SSIM). Nevertheless, even with GRIDL some remaining artifacts are visible in the reconstructed slice.

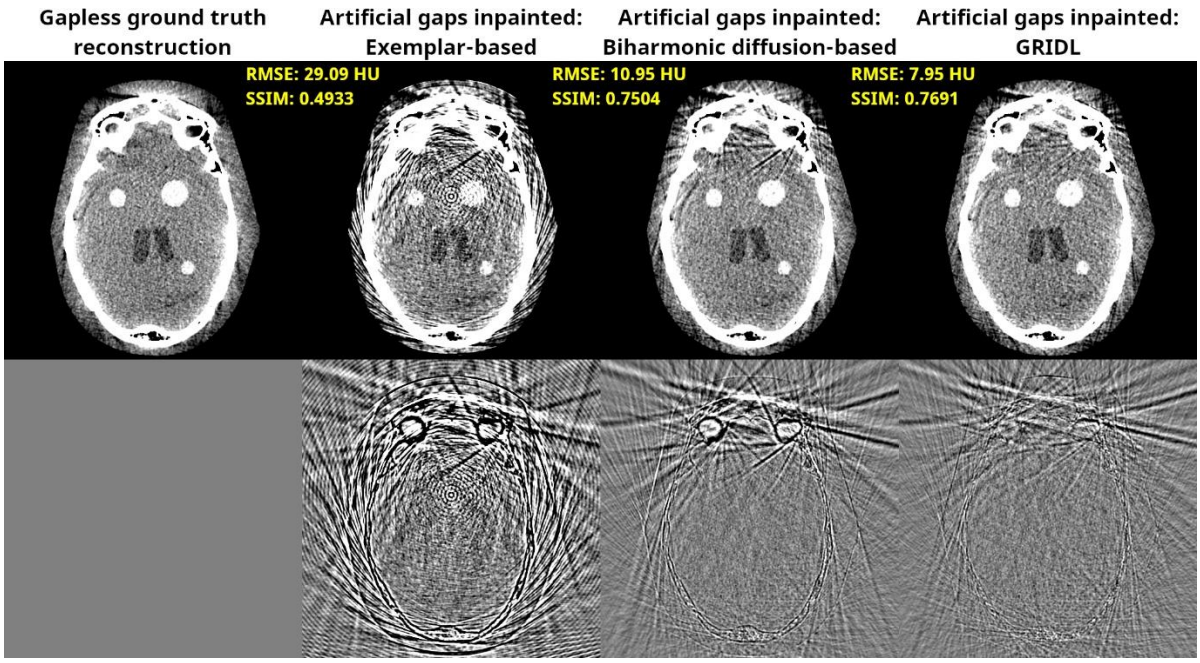

Figure 4: Comparison of inpainting approaches in image domain. Reconstructed images: C = 20 HU, W = 80 HU, difference image: C = 0 HU, W = 70 HU. Reconstructed slice width: 0.75 mm.

Conclusions

In this experimental setup, we evaluated our deep learning-based inpainting approach by applying it to corrupted projection data of an EID. GRIDL successfully inpaints the ASG-like gap pattern in projection data and outperforms the other traditional inpainting approaches in terms of image quality in reconstructed images while reducing artifacts. These results can be seen as a proof of concept. Further research will be focused on the improvement and application of GRIDL to real PCCT projection data.

References

[1] Lell, M. and Kachelrieß, M., "Computed Tomography 2.0: New Detector Technology, AI, and Other Developments," *Invest. Radiol.* 58, 587–601 (08 2023).

[2] Magonov, J., Maier, J., Erath, J., Sunnegårdh, J., Fournié, E., Stierstorfer, K., and Kachelrieß, M., "Reducing Windmill Artifacts in Clinical Spiral CT using a Deep Learning-Based Projection Raw Data Upsampling: Method and Robustness Evaluation," *Med. Phys.* (01 2024).

[3] Magonov, J., Erath, J., Maier, J., Fournié, E., Stierstorfer, K., and Kachelrieß, M., "Deep Learning-Based Detector Row Upsampling for Clinical Spiral CT," *7th International Conference on Image Formation in X-Ray Computed Tomography* 12304, 1230407, International Society for Optics and Photonics, SPIE (10 2022).

[4] Barnes, C., Shechtman, E., Finkelstein, A., and Goldman D. B., "PatchMatch: A Randomized Correspondence Algorithm for Structural Image Editing". *ACM Trans. Graph.* 28(3), (08 2009).

[5] Damelin, S. B. and Hoang, N. S., "On Surface Completion and Image Inpainting by Biharmonic Functions: Numerical Aspects," *Int. J. Math. Math. Sci.* 2018, 1–8 (02 2018).

[6] van der Walt, S., Schönberger, J. L., Nunez-Iglesias, J., Boulogne, F., Warner, J. D., Yager, N., Gouillart, E., and Yu, T., "Scikit-Image: Image Processing in Python," *PeerJ* 2, e453 (06 2014).